J Nanotechnol Nanomaterials. 2022;3(2):90-96.

Journal of Nanotechnology and Nanomaterials Research Article

Electrochemical Supercapacitors Based on Hydrous RuO2/ oxidized Multi-walled Carbon Nanotube Composites

Bo-Kyung Choi[1], Jae-Kyoung Ko[2], Byoung-Suhk Kim[3,*], Min-Kang Seo[1,*]

[1]Korea Carbon Industry Promotion Agency, Jeonju 54853, South Korea

[2]Carbon Composite Energy Nanomaterials Research Center, Woosuk University, Wanju 55338, South Korea

[3]Department of Organic Materials & Fiber Engineering, Jeonbuk National University, Jenoju 567, South Korea

[*]Correspondence should be addressed to Byoung-Suhk Kim, kbsuhk@jbnu.ac.kr; Min-Kang Seo, seomk721@kcarbon.or.kr

Received date: September 01, 2022, **Accepted date:** September 26, 2022

Citation: Choi BK, Ko JK, Kim BS, Seo MK. Electrochemical Supercapacitors Based on Hydrous RuO2/oxidized Multi-walled Carbon Nanotube Composites. J Nanotechnol Nanomaterials. 2022;3(2):90-96.

Abstract

Electrochemical properties of ruthenium oxide (RuO_2)/oxidized multi-walled carbon nanotube (MWCNT) (RuO_2/MWCNT) composite electrodes in supercapacitors were investigated. The electrodes were prepared by impregnating MWCNTs with different concentrations of $RuCl_3 \cdot xH_2O$ solution, followed by chemical reduction and annealing at 150°C under a nitrogen atmosphere. RuO_2 deposited on the MWCNTs was hydrous and amorphous when annealed at 150°C. Transmission electron microscopy (TEM) and Energy dispersive X-ray spectroscopy (EDX) analyses showed that the RuO_2 particles had a uniform size distribution, confirming the presence of RuO_2 in the prepared composites. Cyclic voltammetry analysis suggested that the specific capacitance of the 10 wt% RuO_2/MWCNT composite electrode was significantly higher than those of the pristine MWCNT and 5 wt% RuO_2/MWCNT electrodes in the same medium. This superior performance is probably attributable to the pseudocapacitance of amorphous RuO_2.

Keywords: Electrochemical properties, RuO_2, Multi-walled carbon nanotubes, Supercapacitors

Introduction

Supercapacitors have attracted considerable interest for the fabrication of next-generation energy storage devices because of their high power density, long cyclic life, good safety features, fast charging-discharging processes, and eco-friendly nature [1-5]. Depending on the energy-storage mechanism, there are two types of supercapacitors: electrical double-layer capacitors (EDLCs) and pseudocapacitors. In the former, energy is stored mainly by the virtue of separation of electronic and ionic charges at the interface between the electrode materials and electrolyte solution. In the latter, fast faradaic reactions occur at the electrode materials [6]. Hence, pseudocapacitors should ideally store a higher amount of charge than their EDLC counterparts [7].

Electrode materials with high electrical conductivities, such as carbon black, carbon nanotubes, and carbon fibers [8-11], are generally used as electronic conductors. The supercapacitive behavior of several transition metal oxides, such as RuO_2 [12,13], IrO_2 [14], and NiOx [15], has been extensively studied. Among these, hydrous ruthenium oxide ($RuO_2 \cdot xH_2O$) has been recognized as one of the most promising candidates for active electrode materials because it can store charge by reversibly accepting and donating protons from an aqueous electrolyte. This process is governed by the potential-dependent equilibrium given in Eq. (1) [16,17]:

$$RuOx(OH)y + \delta H+ + \delta e- \rightarrow RuOx-\delta(OH)y+\delta \quad (1)$$

As a result of charge infusion, the oxidation state of Ru for the Ru^{4+}/Ru^{3+} couple is expected to change among +4 (Ru^{4+}), +3 (Ru^{3+}), and +2 (Ru^{2+}), as expressed in Eq. (2).

$$Ru^{4+} - O + H^+ + e^- \rightarrow Ru^{3+} - OH \quad (2)$$

Eqs. (1) and (2) imply that $RuO_2 \cdot xH2O$ is an ionic compound with protons inserted into its lattice. $RuO_2 \cdot xH_2O$ is also a metallic conductor. Cyclic voltammetry (CV) shows a nearly constant current vs. applied voltage and weak evidences of

distinct charge couples, implying that electrons are fully or partially delocalized and that there are no discrete ions [18]. Therefore, hydrous RuO_2 can behave as a mixed electronic-protonic conductor [19,20]. Its electrochemical properties depend on the amount of water incorporated in its structure, and optimum charge storage (pseudocapacitance) is achieved when $RuO_2 \cdot xH_2O$ is heated at ~150°C to yield a compound with $x \approx 0.5$ [21-24].

A review of previous reports indicated that relatively high specific capacitances were obtained particularly when a small amount of RuO_2 was uniformly dispersed on carbonaceous materials with very high surface areas [25,26]. Therefore, highly electroactive transition metal oxide-decorated electrochemically conductive carbonaceous substrates with high specific surface areas are considered promising candidates for improving the capacitive performance of electrode materials. Considerable research has been devoted to achieve enhanced capacitance using multi-walled carbon nanotubes (MWCNTs) functionalized with RuO_2 [27,28].

In this study, we report the pseudocapacitive behavior of oxidized MWCNTs functionalized with hydrous RuO_2 in 1 M sulfuric acid (H_2SO_4) for application in supercapacitors. Our functionalization approach provides an easy way to improve the capacitance of MWCNT with hydrous RuO_2, which is very useful for realizing carbon nanotube-based energy storage materials in the near future. The resulting RuO_2/MWCNT composites were characterized by X-ray diffraction (XRD), TEM with EDX spectroscopy, and particle size distribution (PSD). The electrochemical behavior of the composite electrodes was tested using CV and electrochemical impedance spectroscopy (EIS).

Experimental Procedure

The MWCNTs (purity: > 95%, length: 5–20 μm, diameter: 8–15 nm) used in this work were obtained from Nano Solution Chem. Co., Korea. The details of MWCNT preparation have been discussed elsewhere [29]. $RuCl_3 \cdot xH2O$ (40~49% Ru content, ≤ 0.1% insoluble matter) used in this work was purchased from Sigma-Aldrich. All other chemicals were purchased from Chemical Reagent Co., Ltd. and used as received. As reported earlier [30], for preparing oxidized MWCNTs, the MWCNTs were refluxed with 6 M HNO_3 at 120°C for 3 h to remove metal catalyst impurities and generate oxygenated functional groups on their surface. The oxidized MWCNTs were thoroughly washed with double-distilled water and dried in an oven at 110°C. The oxidized MWCNTs were dispersed in a mixture of isopropanol and water (1:1 volume) by ultrasonic agitation. Then, 5–10 wt.% $RuCl_3 \cdot 2H_2O$ was added to the mixture, which was further ultrasonicated for 1 h. The resultant RuO_2/MWCNTs were filtered and washed thoroughly with doubled distilled water to remove excess chloride ions, and then dried in an oven at 110°C. Finally, the 5 and 10 wt% RuO_2/MWCNT samples were annealed at 150°C under a nitrogen atmosphere. The samples (3 mg) were dispersed in 10 mL of *N,N*-dimethylformamide under ultrasonic agitation. A drop of the mixture was placed on the polished surface of the glassy carbon electrode and dried in an oven at 110°C to evaporate the solvent. A similar procedure was used to prepare the pristine MWCNT electrodes.

XRD measurements were performed on a Rigaku Model D/Max-III B instrument operating at 40 keV and 40 mA using CuK_α radiation. The surface morphologies of the pristine MWCNTs and RuO_2/MWCNT composites were characterized by high-resolution TEM (HR-TEM; JEOL model 2010 TEM using 100 keV beam energy) and EDX spectroscopy (AN-10000/85S EDX spectrometer). Before acquiring the electron micrographs, the samples were ultrasonically dispersed in ethyl alcohol, following which a drop of the resultant dispersion was deposited and dried on a lacey carbon film suspended on a copper grid.

Electrochemical properties of the fabricated electrodes were analyzed in 1 M H_2SO_4 electrolyte using a conventional three-electrode system composed of the prepared RuO_2/MWCNT composite electrode as the working electrode, Ag/AgCl (saturated KCl solution) as the reference electrode, and platinum wire as the counter electrode. Electrochemical measurements were performed using an electrochemical analyzer system (Autolab PGSTAT 30 cyclic voltammetry equipment). The specific gravimetric capacitance, Cg (F/g), was calculated from the gravimetric discharge process according to relation $Cg = i\Delta t_d/\Delta V$, where i is the constant discharge current density (A/g), Δt_d is the discharging time (measured from 0 to 0.9 V), and ΔV is the potential change apart from the ohmic drop. Electrochemical impedance measurements were carried out for both pristine MWCNTs and RuO_2/MWCNT composite samples by applying an AC signal of 10 mV amplitude over a frequency range of 10 mHz–40 kHz.

Results and Discussion

Structural and morphological properties

Because RuO_2 usually exists as hydrates, the precise loading of RuO_2 must be identified on a wet basis. Thus, the loaded amounts of RuO_2 were calculated by considering the weight loss of water measured by thermal analysis, as shown in **Table 1**. Pristine MWCNTs have a specific surface area of 240 m^2/g [29]. As expected, the specific surface area of the RuO_2/MWCNT composites decreases with increasing Ru content. This was attributed to the pore-blocking effect and particle aggregation on the surface of the MWCNTs. In addition, when MWCNTs are used as a support, the effective utility of Ru can be as high as 95% or 96% at high loadings of approximately 4.8% or 9.7%, respectively, which is beneficial for preparing high-loading electrode materials.

Table 1. Loaded amounts of RuO_2 and effective utility ratio of Ru on MWCNTs			
Specimens	S_{BET} (m^2/g)	Utility ratio* (%)	Loaded amounts of Ru (wt%)
pristine MWCNTs	240	-	-
5 wt% RuO_2/MWCNTs	210	95	~4.8
10 wt% RuO_2/MWCNTs	186	96	~9.7
* Utility ratio: effective utility of noble metal Ru			

Figure 1 shows the XRD patterns of the pristine MWCNTs and 5–10 wt% RuO_2/MWCNT composites. The peaks at 26.3°, 43.75°, and 54.70° can be assigned to the (0 0 2), (1 0 0), and (0 0 4) planes of carbon [31,32], respectively, in good agreement with that of the previous literature [33,34]. There is a weak peak from metallic Ru at 38 and no identification of any crystalline phase of RuO_2 in the composites. Moreover, the heights of the (0 0 2) and (1 0 0) peaks are proportional to crystallites sizes L_c (≅2.5 nm) and L_a (≅13.6 nm), respectively [35,36]. However, no Ru peak could be observed, suggesting an amorphous morphology. XRD analysis indicated the reduction of Ru ions in the first stage of the chemical reduction process to crystalline Ru particles and hydrous RuO_2. The redox reaction of RuO_2 dominated the electrochemical reaction when sufficient number of RuO_2 nanoparticles were nucleated by annealing. These results are consistent with the linear sweep voltammetry (LSV) curves, which show oxidation peak currents at 1.0 and 1.2 V, and reduction peak current at −0.35 V. Thus, the following redox reactions can be considered to occur:

$$Ru_2O_3 + H_2O \rightarrow 2RuO_2 + 2H^+ + 2e^- \; E^0 = 0.878 \text{ V}$$

$$Ru^{3+} + e^- \rightarrow Ru^{2+} \; E^0 = 0.878 \text{ V, and}$$

$$Ru^{2+} + 2H_2O \rightarrow RuO_2{\cdot}H_2O + 4H^+ + 2e^- \; E^0 = 0.878 \text{ V}$$

TEM images, particle size distribution, and EDX analysis of pristine MWCNTs and the 10 wt% RuO_2/MWCNT composite are shown in **Figure 2**. TEM images indicated that RuO_2 nanoparticles were highly dispersed and well anchored on the surfaces of the MWCNTs, forming a randomly entangled network compared to that in the pristine MWCNTs. The TEM image (**Figure 2b**) reveals that the MWCNTs were covered by RuO_2 nanoparticles. No separate aggregation of the RuO_2 nanoparticles was observed, indicating that nucleation was effectively limited to the surface of the MWCNTs. **Figure 2c** clearly shows MWCNTs with conical herringbone structures. Most of the nanoparticles were settled on the external surface of the herringbone-structured MWCNTs. However, some nanoparticles tend to enter the cavities of the nanotubes from the open ends because of the smaller sizes compared to the inner diameter of the MWCNTs and the low surface tension of water. The HRTEM image (**Figure 2c**) also reveals that the RuO_2 nanoparticles do not have a distinct crystal structure. This indicates that the RuO_2 nanoparticles are in an amorphous state, which is in good agreement with the XRD patterns shown in **Figure 1**. Meanwhile, the crystal structure of the MWCNTs remained unchanged, indicating that the deposition of RuO_2 did not affect the crystallinity of the MWCNTs. The size distribution of the supported **RuO_2** nanoparticles was evaluated from the statistical measurements of 500 randomly selected particles (**Figure 2d**). These particle sizes are in the range of 0.8–3 nm, with an average size of ~1.6 nm.

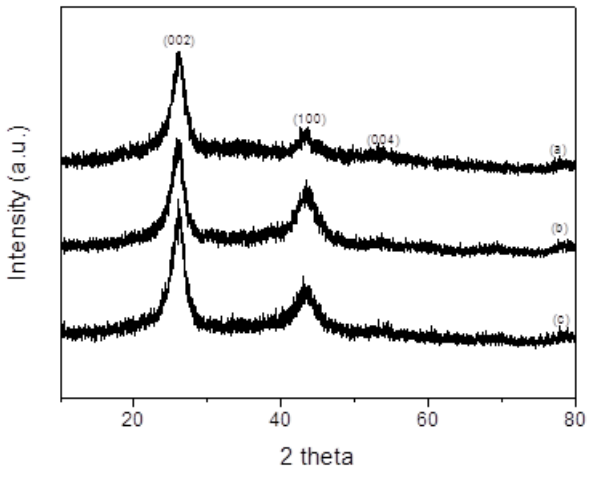

Figure 1. XRD spectra of (a) pristine MWCNTs, (b) 5 wt% RuO_2/MWCNT composite, and (c) 10 wt% RuO_2/MWCNT composite.

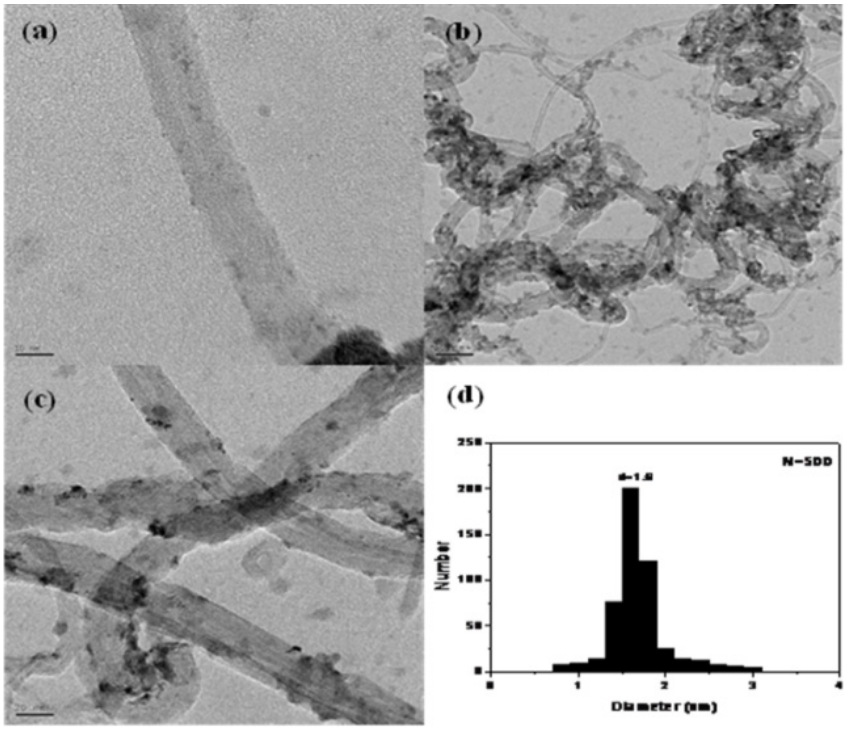

Figure 2. TEM and PSD of pristine MWCNTs and 10 wt% RuO_2/MWCNT composites: **(a)** pristine MWCNTs, **(b)** low magnification, **(c)** high magnification, and **(d)** particle size distribution.

The 10 wt% RuO_2/MWCNT composite was further characterized using EDX to examine the chemical composition. The EDX spectrum (**Figure 3**) shows that the 10 wt% RuO_2/MWCNT composite is composed of Ru, O, and C. The Cu peak was attributed to the Cu microgrid on which the product was loaded. Based on the electron microscopy analysis, it is reasonable to conclude that the RuO_2 nanoparticles are well anchored on the surfaces of the MWCNTs, yielding carbon nanocomposites that can be applied to supercapacitors.

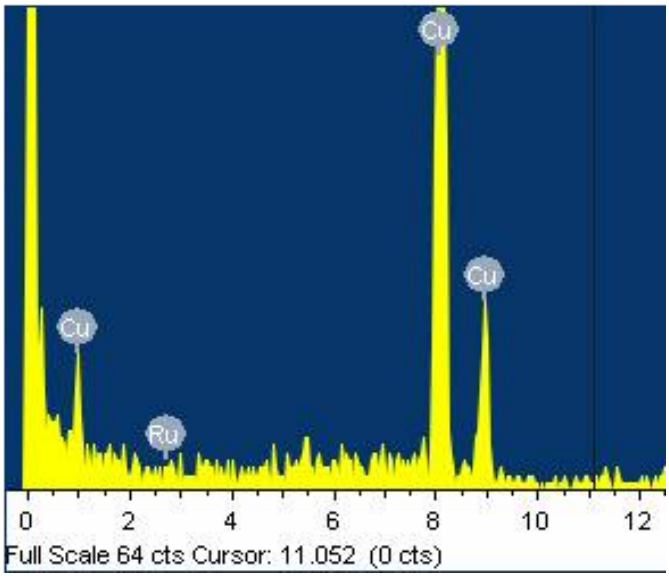

Figure 3. EDX spectrum of the 10 wt% RuO_2/MWCNT composite.

Electrochemical properties

CV curves were acquired at a scan rate of 50 mV/s to investigate the influence of RuO_2 deposition on the capacitance of the fabricated composite electrodes. **Figure 4** displays the CV curves of the pristine MWCNTs and 5–10 wt% RuO_2/MWCNT composite electrodes in 1 M H_2SO_4. The peaks at 0.08 V (anodic) and 0.13 V (cathodic) vs. Ag/AgCl are associated with oxygen-containing surface functionalities such as carboxylic acids on the surfaces of the MWCNTs. Another redox pair is observed at 0.52 and 0.58 V for anodic and cathodic potentials vs. Ag/AgCl, respectively. All these peaks indicate the presence of oxygenated functional groups, as they exhibit pH-dependent behavior. These peaks are attributed to oxygenated surface functionalities such as quinones and functional groups that show peaks similar to those of glassy carbon electrodes [37,38].

The cathodic peak shifted negatively with increasing RuO_2 content, whereas the anodic peak shifted positively. This may be due to the high packing density of the MWCNTs, which is considerably smaller than the thickness of the diffusion layer of the electrolyte, thus leading to semi-infinite planar diffusion that is similar to the case of planar macroelectrodes. The specific capacitance essentially depends on the microtexture of the nanotubes, number of defects, micropore volume, and catalyst contamination. The accumulation of charges in the electrode-electrolyte interface mainly depends on the accessibility of electrolyte ions to the sidewalls and the central core of the nanotubes. Open tips, number of defects, and presence of an interconnected network can also result in enhanced capacitance. The gravimetric capacitance of the 10 wt% RuO_2/MWCNT composite is 130 F/g in the linear region of the voltammogram, where the MWCNTs show an ideal double-layer capacitive behavior.

Electrochemical impedance was investigated to characterize the capacitive performance. **Figure 5** shows the complex plane plots of the impedance of the 10 wt% RuO_2/MWCNT composite in 1 M H_2SO_4. Impedance spectroscopy is a valuable tool not only for determining the equivalent series resistance but also for studying the interfacial and pseudocapacitance behaviors of the electrode. In this technique, an alternating voltage is applied to the electrode interface; the response is represented by an imaginary component, Z″, of the impedance, which is the capacitance of the electrode given by the equation $Z'' = 1/j\omega C$. The internal impedance involves two mechanisms, including the resistances of mass transport and the electrode materials [39]. In our experiment, the mass-transport resistance of the electrolyte was almost constant. This value represents the performance of the electrode materials.

The impedance plots can be divided into high- and low-frequency regions, as shown in **Figure 5.** The frequency at which there is deviation from the semicircle is known as the 'knee' frequency, and it reflects the maximum frequency at which the capacitive behavior is dominant. The larger semicircle in the high-frequency region for the RuO_2/MWCNTs suggests the existence of charge transfer resistance (R_{CT}). MWCNTs [40] exhibit a small semicircle in the high-frequency region, whereas a straight line inclined at more than 45° to the real axis can be observed in the low-frequency region. This behavior can be attributed to the porous nature of the MWCNTs. The central hollow core of the nanotubes is accessible for double-layer charging, and thus the open MWCNTs act as a condenser for the accumulation of charges. Deviations from this behavior were observed for the 10 wt% RuO_2/MWCNT composite, as indicated by the large semicircle. This was due to the presence of RuO_2 on the MWCNTs, which offered resistance to the diffusion of electrolyte ions within

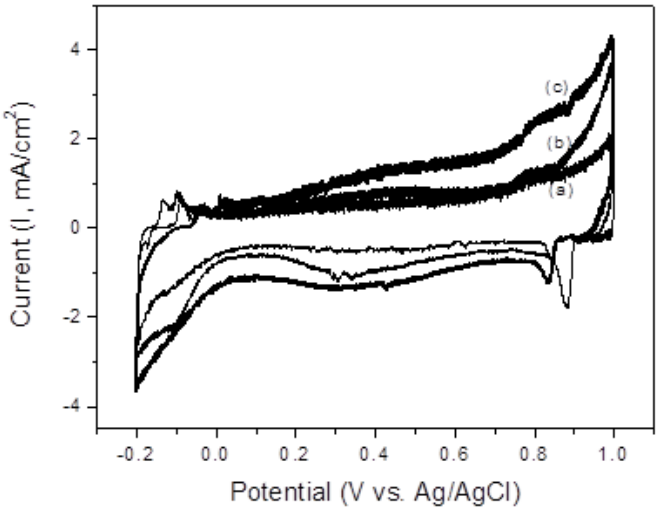

Figure 4. CV curves of **(a)** pristine MWCNTs, **(b)** 5 wt% RuO_2/MWCNT composite, and **(c)** 10 wt% RuO_2/MWCNT composite in 1 M H_2SO_4 (scan rate: 50 mV/s).

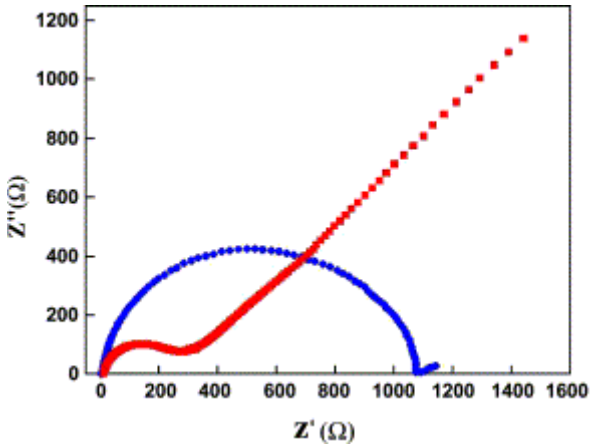

Figure 5. Complex plane impedance plots of pristine MWCNT (red) and 10 wt% RuO_2/MWCNT composite (blue) in 1 M H_2SO_4.

the pores of the nanotubes. Although the model-dependent capacitance obtained from the impedance spectrum is considerably lower than the capacitance obtained from the voltammetric data, enhancement of the capacitance by an order of magnitude suggests a positive role of the Ru species introduced on the MWCNTs.

Conclusions

The inherent electrochemical capacitance of the RuO_2/MWCNT composite electrodes was significantly enhanced upon functionalization by hydrous RuO_2. Oxidative treatment of the MWCNTs generated oxygen-containing functional groups at the defective sites, which could be further derivatized by hydrous RuO_2. Owing to its pseudocapacitive behavior, RuO_2 significantly increased the capacitance of the RuO_2/MWCNT composite electrodes. Furthermore, a higher RuO_2 content resulted in an increased specific capacitance that was derived from the pseudocapacitance of RuO_2. Notably, the 10 wt% RuO_2/MWCNT composite electrodes showed the highest specific capacitance, largely due to an increase in the equivalent series resistance and overall capacitance.

Acknowledgments

This research was supported by National Standard Technology Improvement Project (20011582) through the Korea Evaluation Institute of Industrial Technology (KEIT) funded by the Ministry of Trade, Industry & Energy (MOTIE, Korea).

References

1. Hu CC, Chen WC. Effects of substrates on the capacitive performance of RuOx· nH2O and activated carbon–RuOx electrodes for supercapacitors. Electrochimica Acta. 2004 Sep 1;49(21):3469-77.

2. Ruiz V, Blanco C, Granda M, Santamaría R. Enhanced life-cycle supercapacitors by thermal treatment of mesophase-derived activated carbons. Electrochimica Acta. 2008 Dec 30;54(2):305-10.

3. Kormann M, Gerhard H, Popovska N. Comparative study of carbide-derived carbons obtained from biomorphic TiC and SiC structures. Carbon. 2009 Jan 1;47(1):242-50.

4. Staiti P, Lufrano F. Study and optimisation of manganese oxide-based electrodes for electrochemical supercapacitors. Journal of Power Sources. 2009 Feb 1;187(1):284-9.

5. Lv G, Wu D, Fu R, Zhang Z, Su Z. Electrochemical properties of conductive filler/carbon aerogel composites as electrodes of supercapacitors. Journal of Non-crystalline Solids. 2008 Oct 15;354(40-41):4567-71.

6. Fan Z, Chen J, Cui K, Sun F, Xu Y, Kuang Y. Preparation and capacitive properties of cobalt–nickel oxides/carbon nanotube composites. Electrochimica Acta. 2007 Feb 15;52(9):2959-65.

7. Song RY, Park JH, Sivakkumar SR, Kim SH, Ko JM, Park DY, et al. Supercapacitive properties of polyaniline/Nafion/hydrous RuO2 composite electrodes. Journal of Power Sources. 2007 Mar 30;166(1):297-301.

8. Hu CC, Chang KH, Lin MC, Wu YT. Design and tailoring of the nanotubular arrayed architecture of hydrous RuO2 for next generation supercapacitors. Nano Letters. 2006 Dec 13;6(12):2690-5.

9. Taberna PL, Chevallier G, Simon P, Plée D, Aubert T. Activated carbon–carbon nanotube composite porous film for supercapacitor applications. Materials Research Bulletin. 2006 Mar 9;41(3):478-84.

10. Seo MK, Park SJ. Electrochemical characteristics of activated carbon nanofiber electrodes for supercapacitors. Materials Science and Engineering: B. 2009 Aug 25;164(2):106-11.

11. Seo MK, Park SJ. Influence of air-oxidation on electric double layer capacitances of multi-walled carbon nanotube electrodes. Current Applied Physics. 2010 Jan 1;10(1):241-4.

12. Conway BE. Electrochemical supercapacitors: scientific fundamentals and technological applications. Plenum, New York: Kluwer Academic; 1999.

13. Miller JM, Dunn B. Morphology and electrochemistry of ruthenium/carbon aerogel nanostructures. Langmuir. 1999 Feb 2;15(3):799-806.

14. Hu CC, Huang YH, Chang KH. Annealing effects on the physicochemical characteristics of hydrous ruthenium and ruthenium–iridium oxides for electrochemical supercapacitors. Journal of Power Sources. 2002 Jun 1;108(1-2):117-27.

15. Nam KW, Kim KB. A study of the preparation of NiO x electrode via electrochemical route for supercapacitor applications and their charge storage mechanism. Journal of the Electrochemical Society. 2002 Feb 7;149(3):A346-54.

16. Trasatti S, editor. Electrodes of conductive metallic oxides. London: Elsevier; 1980.

17. Trasatti S. Physical electrochemistry of ceramic oxides. Electrochimica Acta. 1991 Jan 1;36(2):225-41.

18. Fletcher JM, Gardner WE, Greenfield BF, Holdoway MJ, Rand MH. Magnetic and other studies of ruthenium dioxide and its hydrate. Journal of the Chemical Society A: Inorganic, Physical, Theoretical. 1968:653-7.

19. Dmowski W, Egami T, Swider-Lyons KE, Love CT, Rolison DR. Local atomic structure and conduction mechanism of nanocrystalline hydrous RuO2 from X-ray scattering. The Journal of Physical Chemistry B. 2002 Dec 12;106(49):12677-83.

20. McKeown DA, Hagans PL, Carette LP, Russell AE, Swider KE, Rolison DR. Structure of hydrous ruthenium oxides: implications for charge storage. The Journal of Physical Chemistry B. 1999 Jun 10;103(23):4825-32.

21. Zheng JP, Cygan PJ, Jow TR. Hydrous ruthenium oxide as an electrode material for electrochemical capacitors. Journal of the Electrochemical Society. 1995 Aug 1;142(8):2699-2730.

22. Mills A, Giddings S, Patel I, Lawrence C. Thermally activated ruthenium dioxide hydrate. A reproducible, stable oxygen catalyst. Journal of the Chemical Society, Faraday Transactions 1: Physical Chemistry in Condensed Phases. 1987;83(8):2331-45.

23. Kim IH, Kim JH, Kim KB. Electrochemical characterization of electrochemically prepared ruthenium oxide/carbon nanotube electrode for supercapacitor application. Electrochemical and Solid-State Letters. 2005 May 24;8(7):A369-72.

24. Chang KH, Hu CC, Chou CY. Textural and Capacitive Characteristics of Hydrothermally Derived RuO2·xH2O Nanocrystallites: Independent Control of Crystal Size and Water Content. Chemistry of Materials. 2007 Apr 17;19(8):2112-9.

25. Fu X, Yu H, Peng F, Wang H, Qian Y. Facile preparation of RuO2/CNT catalyst by a homogenous oxidation precipitation method and its catalytic performance. Applied Catalysis A: General. 2007 Apr 11;321(2):190-7.

26. Over H, Kim YD, Seitsonen AP, Wendt S, Lundgren E, Schmid M, et al. Atomic-scale structure and catalytic reactivity of the RuO2 (110) surface. Science. 2000 Feb 25;287(5457):1474-6.

27. Andrews R, Jacques D, Rao AM, Derbyshire F, Qian D, Fan X, et al. Continuous production of aligned carbon nanotubes: a step closer to commercial realization. Chemical Physics Letters. 1999 Apr 16;303(5-6):467-74.

28. Fang WC, Chyan O, Sun CL, Wu CT, Chen CP, Chen KH, et al. Arrayed CNx NT–RuO2 nanocomposites directly grown on Ti-buffered Si substrate for supercapacitor applications. Electrochemistry Communications. 2007 Feb 1;9(2):239-44.

29. Yang ZH, Wu HQ. The electrochemical impedance measurements of carbon nanotubes. Chemical Physics Letters. 2001 Aug 3;343(3-4):235-40.

30. Seo MK, Saouab A, Park SJ. Effect of annealing temperature on electrochemical characteristics of ruthenium oxide/multi-walled carbon nanotube composites. Materials Science and Engineering: B. 2010 Feb 25;167(1):65-9.

31. Qu D. Studies of the activated carbons used in double-layer supercapacitors. Journal of Power Sources. 2002 Jul 1;109(2):403-11.

32. Liu X, Yang Y, Liu H, Ji W, Zhang C, Xu B. Carbon nanotubes from catalytic pyrolysis of deoiled asphalt. Materials Letters. 2007 Jul 1;61(18):3916-9.

33. Gobal F, Faraji M. RuO 2/MWCNT/stainless steel mesh as a novel positive electrode in vanadium redox flow batteries. RSC Advances. 2015;5(84):68378-84.

34. Zhang B, Xu Y, Zheng Y, Dai L, Zhang M, Yang J, et al. A facile synthesis of polypyrrole/carbon nanotube composites with ultrathin, uniform and thickness-tunable polypyrrole shells. Nanoscale Research Letters. 2011 Dec;6(1):1-9.

35. Warren BE. X-ray diffraction in random layer lattices. Physical Review. 1941 May 1;59(9):693-8.

36. Saenko NS. The X-ray diffraction study of three-dimensional disordered network of nanographites: experiment and theory. Physics Procedia. 2012 Jan 1;23:102-5.

37. Seo MK, Park SJ. Effect of nanosize titanium oxide on electrochemical characteristics of activated carbon electrodes. Current Applied Physics. 2010 Mar 1;10(2):391-4.

38. Seo MK, Yang S, Kim IJ, Park SJ. Preparation and electrochemical characteristics of mesoporous carbon spheres for supercapacitors. Materials Research Bulletin. 2010 Jan 1;45(1):10-4.

39. Musić S, Popović S, Maljković M, Furić K, Gajović A. Influence of synthesis procedure on the formation of RuO2. Materials Letters. 2002 Nov 1;56(5):806-11.

40. Lee JK, Pathan HM, Jung KD, Joo OS. Electrochemical capacitance of nanocomposite films formed by loading carbon nanotubes with ruthenium oxide. Journal of Power Sources. 2006 Sep 22;159(2):1527-31.